



OPEN Dynamic [^{99m}Tc]Tc-mebrofenin SPECT/CT in preoperative planning of liver resection: a prospective study

Annamária Bakos¹✉, László Libor², Szabolcs Urbán¹, Tibor Géczy², Mátyás Bukva³, József Hóhn², György Lázár², András Nagy⁴, István Farkas¹, Gábor Sipka¹, László Pávics¹ & Zsuzsanna Besenyi¹

Background At least 20% of the future liver remnant must function properly after liver tumor resection to avoid post-hepatectomy liver failure (PHLF). [^{99m}Tc]Tc-mebrofenin scintigraphy and SPECT are unique noninvasive, quantitative methods for evaluating liver function via hepatocellular bilirubin clearance.

Aim To evaluate the value of dynamic [^{99m}Tc]Tc-mebrofenin SPECT/CT parameters for predicting clinically relevant PHLF according to the ISGLS criteria.

Methods Thirty-five patients underwent dynamic [^{99m}Tc]Tc-mebrofenin SPECT/CT imaging to determine the FLR volumetric rate, functional volume rate, total liver filtration and FLR filtration. On the same day, two-dimensional ultrasound shear wave elastography (2D-SWE) was used to assess parenchymal fibrosis in the FLR. The quantitative dynamic SPECT parameters were compared with the relevant clinical scores and ICG.

Results The total liver filtration was inversely correlated with the ICG-R15 and MELD-Na score.

Twenty-four patients underwent major liver resection due to an adequate FLR rate and did not die within 90 days after the procedure. ROC analysis revealed that the FLR filtration was a significant predictor of PHLF. The best cutoff value for FLR filtration was 2.72%/min/m².

Conclusion Dynamic [^{99m}Tc]Tc-mebrofenin SPECT/CT is an essential tool for selecting patients at risk of clinically relevant PHLF after liver resection.

Keywords [^{99m}Tc]Tc-mebrofenin, Hepatectomy, Liver failure, Volumetry, Liver function, Hepatocyte, Metabolic activity

Liver resection is commonly performed and can potentially cure a variety of primary and secondary hepatic malignancies. Currently, post-hepatectomy liver failure (PHLF) is a serious complication of major hepatectomy, with a reported incidence ranging from 9 to 30% in cases of extended resection¹.

The cause of PHLF can be primary or secondary. Intrinsic liver factors and the surgery itself are considered primary causes, whereas postoperative complications and systemic factors (e.g., systemic infections, respiratory complications, and adverse effects of pre- or postoperative drug use) are considered secondary causes².

An insufficient future liver remnant (FLR) is considered one of the main causes of primary PHLF. To prevent or reduce the incidence of liver complications following hepatectomy, accurate assessments of preoperative liver function and FLR volume are essential. Additionally, precise delineation of hepatectomy indications and careful selection of patients who are most likely to benefit from parenchyma modulation techniques, such as portal vein embolization (PVE), portal vein ligation (PVL) or associated liver partition and portal vein ligation for staged hepatectomy (ALPPS), are also important¹.

Total liver function can be assessed via the indocyanine green (ICG) clearance test and several other laboratory and clinical tests³. While these methods offer insight into the global functional status of the liver, they are limited in providing detailed information about the function of individual liver segments. This limitation is particularly relevant in understanding the function of individual future remnant liver segments before resection.

¹Department of Nuclear Medicine, University of Szeged, Szeged, Hungary. ²Department of Surgery, University of Szeged, Szeged, Hungary. ³Department of Immunology, Albert Szent-Györgyi Medical School, Faculty of Science and Informatics, University of Szeged, Szeged, Hungary. ⁴Department of Radiology, University of Szeged, Szeged, Hungary. ✉email: bakos.annamaria@med.u-szeged.hu

Furthermore, two-dimensional ultrasound shear wave elastography (2D-SWE) can diagnose liver fibrosis as well as predict complications⁴, but it cannot provide volumetric information.

Currently, FLR volume is measured via computed tomography (CT) volumetry, which is a well-established method. However, the extent of resection margins varies depending on parenchymal status and factors related to liver function. In most medical centers, patients with a normal liver parenchyma need a FLR volume of at least 25% following major resection, whereas patients with a disease affecting the liver parenchyma need an FLR volume greater than 30%. For individuals presenting with cirrhosis, FLR volumes greater than 40% usually mandate major resection^{5–10}.

Functional volumetry can be assessed via [^{99m}Tc]Tc-mebrofenin hepatobiliary scintigraphy with SPECT, which has been proven reliable for predicting PHLF and measuring not only overall liver function but also regional distribution within the liver. This is particularly important in cases of inhomogeneous distribution of function, such as after liver parenchyma modulation strategies (for example, PVE and ALPPS), and in patients with cirrhosis^{1,11,12}.

Dynamic SPECT imaging allows the visualization of radiopharmaceutical changes in 3D over time¹³. To our knowledge, dynamic three-dimensional (SPECT) methods have not yet been used in the quantitative assessment of future liver remnant function.

Furthermore, methods to determine clinically relevant PHLF in the preoperative period are limited¹⁴.

Objective

The objective of our prospective study was to assess the functional parameters derived from dynamic [^{99m}Tc]Tc-mebrofenin SPECT/CT using our new methodology, with a focus on determining global liver function, FLR function, and the FLR functional rate. Furthermore, the goal is to predict clinically relevant PHLF on the basis of the criteria established by the International Study Group of Liver Surgery (ISGLS).

Materials and methods

From January 2022 to August 2023, 35 patients were recruited for this prospective study, which was conducted in the Department of Surgery at our University. The **inclusion criteria** were as follows: patients scheduled for major liver resection (characterized by the removal of three or more continuous Couinaud segments), with clinically confirmed compensated liver function (based on the MELD-Na score, APRI, Child-Pugh-Turcotte score, and ICG-R15)³ and no anesthesia-related contraindications for surgery. Patient demographics, tumor type, and procedural details were collected prospectively.

Evaluation of total liver function

The APRI, MELD-Na score, Child-Turcotte-Pugh classification and indocyanine green (ICG) clearance test results were assessed prior to major liver resection³. Assessments of the laboratory parameters relevant for calculating the previously mentioned scores, ICG measurement, and dynamic [^{99m}Tc]Tc-mebrofenin SPECT/CT scan were conducted in the same week.

Liver fibrosis measurement: two-dimensional shear wave elastography (2D-SWE)

The liver fibrosis grade was assessed via 2D-SWE. On the day of the dynamic [^{99m}Tc]Tc-mebrofenin SPECT/CT examination, ultrasound shear wave elastography (SWE) with a LOGIQ E9 device (GE HealthCare, USA) was used to measure the elasticity of the FLR to determine the degree of parenchymal fibrosis and the Metavir score. In 2D-SWE, a perpendicular stress force is applied to the liver tissue to induce shear, after which the shear wave velocity is measured. The assessment was deemed successful if there were at least ten successful measurements and if the interquartile range (IQR) did not exceed 30% of the median. Patients were assessed in the supine position with the right arm positioned above the head. During the measurement, patients were instructed to maintain semi-restrained breathing, avoiding both the Valsalva maneuver and deep inhalation. The elastic imaging box was carefully positioned over a homogeneously isoechoic part of the liver parenchyma, which was located at least 2 cm deep to the liver capsule, to avoid blood vessels, bile ducts, and tumor tissues. After the elastic imaging box was completely and evenly filled with color, the area of interest (2 cm in diameter) was plotted, and measurements were taken according to the manufacturer's recommendation. The values are expressed in meters per second (m/s).^{4,15} Among the 35 patients included in the study, 31 patients were able to measure liver elasticity according to the criteria mentioned above.

Dynamic [^{99m}Tc]Tc-mebrofenin SPECT/CT imaging and data acquisition

All 35 patients were required to fast for 4 h before the scan, and the radiopharmaceutical was always prepared onsite on the day of SPECT imaging^{16,17}. All scans were performed on a three-headed integrated SPECT/CT system with a low-energy, high-resolution parallel-hole collimator (Mediso AnyscanTRIO, Mediso Medical Imaging Systems Ltd., Budapest, Hungary) 360°; 96 projections, 6 s/frame, matrix 128 × 128, reconstructed pixel size 4.22 mm. The energy window was positioned on the photon peak of ^{99m}Tc (140 keV) at 20%. Low-dose CT was performed for anatomical mapping and attenuation correction (120 kV and 70 mA·s). During the examination, patients were in the supine position with a field-of-view (FOV) over the liver and heart regions. The FOV included the heart, liver and bile ducts up to the choledochus in all patients. The radiopharmaceuticals were administered intravenously with the arm positioned outside the FOV to prevent interference.

Acquisition

Dynamic SPECT imaging was performed after intravenous administration of [^{99m}Tc]Tc-mebrofenin 300 MBq with a 192-second frequency acquisition time in continuous mode according to the Mediso basic setup. Immediately after the radiotracer was injected and tracer inflow was detected in the aorta, continuous successive

3D (SPECT) scans were performed to continuously monitor the radiotracer. In this way, the dynamic SPECT scans include the liver uptake phase, which involves the extraction of the tracer from the blood into hepatocytes, the subsequent accumulation of the tracer in hepatocytes, and the biliary excretion phase with continuous data acquisition. The values obtained from continuous 3D acquisition are used to fit the time-activity curve, which can be determined from the VOIs accurately determined via SPECT. During the examination, a total of 20 SPECT scans were performed from the time of radiopharmaceutical administration. (Fig. 1).

Imaging analysis

On the SPECT scan, the volume of interest (VOI) was manually drawn around the heart and large vessels in the mediastinum (serving as the blood pool, BP), liver, FLR and total field-of-view (FOV). The VOI was carefully positioned around the blood pool and liver regions to avoid overlap and incorrect summation of hepatic and cardiac activity. To delineate the VOI around the blood pool, the scattering caused by the left lobe of the liver should be considered and there should be no plotting in the right ventricle. The VOI of the liver was manually edited by the user on a slice-by-slice basis to correct for over- or underestimation. This ensures that only functional hepatocyte activities are included in the liver VOI and the FLR VOI. The total FOV, which includes the definition of total body activity, was automatically drawn. (Fig. 1).

Time-activity curves (TACs) were generated for each source organ: blood pool, whole liver, future liver remnant (FLR), and total field-of-view (FOV) (Fig. 1). TACs were generated by fitting biexponential functions via nonlinear least-squares minimization with the Levenberg-Marquardt algorithm, as implemented via the open-source fitting package *lmfit* (version 1.2.2)¹⁸.

Total liver filtration (TL-F, %/min) and future liver remnant filtration (FLR-F, %/min) were calculated from the generated time-activity curves at time intervals between 150 and 350 s post injection according to Ekman's formula¹⁹. Total liver filtration and future liver remnant filtration (FLR-F) were normalized to body surface area (BSA, %/min/m²) to account for individual metabolic rates and were calculated via the Mosteller formula²⁰.

Determine FLR-functional volume rate (FLR-FV%) and FLR-volume rate (FLR-V%)

In the early, purely parenchymal phase SPECT scan, where biliary excretion did not appear, the FLR functional volume rate (FLR-FV%) was calculated as the ratio of the sum of the voxel counts of the future liver remnant (FLR-C) to the sum of the voxel counts of the total liver (TL-C) and expressed as a percentage after multiplying by 100. No biliary tracer activity was visible on these SPECT images during this period. The future liver residual

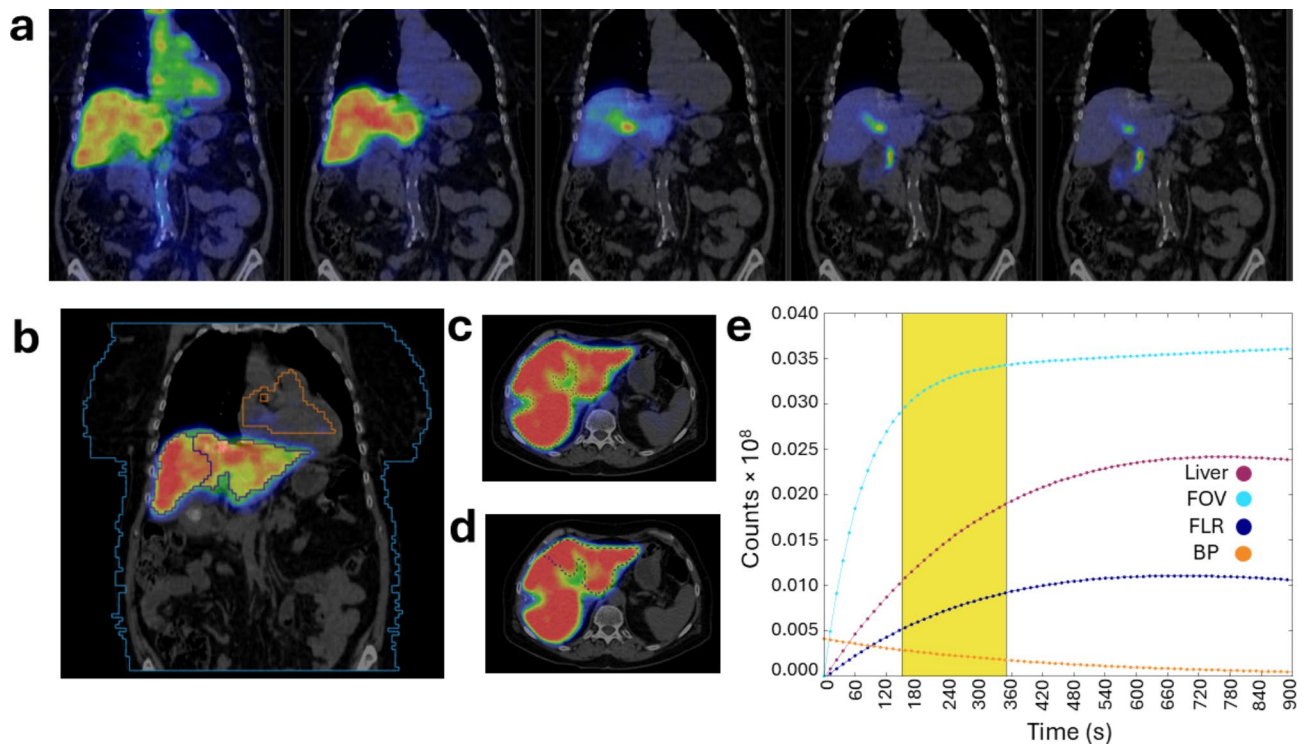


Fig. 1. Dynamic [^{99m}Tc]Tc-mebrofenin SPECT/CT results.

a: Coronal slices of the total field of view. First 5 SPECT scans.

b: Coronal slice of the total field of view with the VOI regions in the parenchymal phase.

c: Representative transverse SPECT/CT image of a liver with a liver VOI in the parenchymal phase.

d: Representative transverse SPECT/CT image of a liver with the FLR VOI in the parenchymal phase.

e: Time-activity curves according to the VOI regions. The time intervals marked in yellow are used to determine filtration.

volume fraction (FLR-V%) was calculated as the ratio of the FLR volume (FLR-V) to the tumor-free total liver volume (TL-V) and expressed as a percentage after multiplication by 100.

All patients had previously undergone a contrast-enhanced CT or MRI scan as a part of the staging examination. For accurate determination of the liver resection line, a previous (within 2 weeks) contrast-enhanced CT or MRI scan was used as a reference for the SPECT/CT images.

Different cutoff values were used to determine the rate of FLR sufficient to perform the planned liver resection. In healthy livers, the FLR rate was considered adequate to proceed with planned hepatectomy higher than 25%; in patients having received chemotherapy, the FLR rate was > 30%; and in patients with cirrhosis, the sufficient FLR rate was higher than 40%¹. In addition to the volumetric ratio, the functional FLR ratio was the decisive value. The FLR filtration values were not used in the decision, as this was determined according to a new method (from 3D dynamic SPECT data).

Control dynamic [^{99m}Tc]Tc-mebrofenin SPECT/CT

In thirteen of the 35 patients involved, according to the first dynamic [^{99m}Tc]Tc-mebrofenin SPECT/CT examination, the FLR ratio was less than the desired value, and a parenchymal modulation procedure was performed to perform the surgery, followed by a control study (dynamic [^{99m}Tc]Tc-mebrofenin SPECT/CT) using the same acquisition parameters.

After parenchymal modulation, the control examination was as follows: 6–8 weeks after portal vein embolization (PVE) or portal vein ligation (PVL) and 10–14 days after associating liver partition and portal vein ligation for staged hepatectomy (ALPPS).

Definition of post-hepatectomy liver failure (PHLF)

The established method for measuring postoperative outcomes is the determination of the PHLF grade according to the International Study Group of Liver Surgery (ISGLS)²¹. Grade A PHLF is characterized by abnormal postoperative laboratory parameters that do not require changes in the clinical management of the patient. Grade B PHLF requires deviation from the regular clinical management but no need for invasive treatment. Grade C PHLF requires invasive treatment. Grades B and C were considered clinically relevant liver failure in our study¹⁴.

Patients having received chemotherapy

The term -patients having received chemotherapy- refers to patients who have received at least 3–6 months of intensive preoperative chemotherapy (oxaliplatin-based chemotherapy or irinotecan-based chemotherapy). Liver resection was performed 4–6 weeks after the last cycle of chemotherapy, which according to the literature significantly increases the risk of PHLF²².

Morbidity

Morbidity was assessed according to the Clavien-Dindo classification of surgical complications²³.

Mortality

Mortality was defined as death from any cause during the 90-day postoperative period.

Statistical analyses

For the continuous variables, the median and interquartile range (IQR) were used as measures of central tendency, as these variables mostly followed a right-skewed distribution.

To assess the relationships between continuous variables, we employed Spearman's rank correlation analysis, the results of which are expressed in terms of the ρ correlation coefficient. Spearman's correlation analysis was chosen because most variables did not exhibit a normal distribution. For the variables showing significant correlation, the relationship was illustrated via scatterplots, to which a locally estimated scatterplot smoothing (LOESS) function was fitted to visualize the nonparametric relationship.

The Wilcoxon signed-rank test was used to evaluate changes in continuous variables before and after parenchymal modulation. For unpaired measurements, the Mann-Whitney test was used.

In the receiver operating characteristic (ROC) analyses, the predictive efficiency of each variable was characterized by sensitivity, specificity, positive/negative predictive values, and the area under the curve (AUC), along with the corresponding standard error (SE) and 95% confidence interval (95% CI). The optimal cutoff value was determined using the Youden index.

A p value < 0.05 indicated statistical significance. Statistical analyses were performed using RStudio (2023.12.0 + 369) (ggplot2, ggpubr, cowplot, and dplyr packages).

Results

The demographic and perioperative characteristics of the enrolled patients are summarized in Table 1.

Correlation with total liver function parameters in enrolled patients

We began by assessing the validity of the functional parameters derived from our dynamic SPECT/CT methodology. In order to do this, we analyzed the correlations between total liver filtration values obtained from dynamic [^{99m}Tc]Tc-mebrofenin SPECT/CT and traditional liver function tests, such as the MELD-Na score, APRI, Child-Turcotte-Pugh classification, and ICG-R15. This step was crucial to determine whether our new imaging-based parameters align with established measures of liver function, thereby validating their clinical relevance.

Variable	Value
Basic demographics	Patients (<i>n</i> = 35)
Sex (M/F)	21/14
Age (years, median, IQR)	66.70 (53.4–78.20)
BMI (kg/m ² , median, IQR)	27.80 (24.97–31.14)
Preoperative clinical scores	
MELD-Na (median, IQR)	8.00 (6.00–10.00)
APRI (median, IQR)	0.40 (0.20–0.70)
CTP (median, IQR)	5.00 (5.00–5.00)
ICG-R15 (median, IQR)	5.9 (3.05–7.95)
Patients having received chemotherapy (%)	26 (74%)
Patients with Oxaliplatin-based chemotherapy	20
Patients with Irinotecan-based chemotherapy	6
Patients with Cirrhosis (%)	4 (11%)
FLR Metavir Score by ultrasound 2D-SWE	Patients (<i>n</i> = 31)
F0	9
F1	1
F2	13
F3	4
F4	4
Tumor	Patients (<i>n</i> = 35)
Neuroendocrine tumor metastasis (%)	1 (2.9%)
Colorectal carcinoma metastasis (%)	13 (37.1%)
HCC (%)	8 (22.8%)
IHCC (%)	6 (17.1%)
Renal cell carcinoma metastasis (%)	1 (2.9%)
Squamous cell carcinoma metastasis (%)	2 (5.7%)
Gallbladder carcinoma (%)	2 (5.7%)
Hemangioma (%)	1 (2.9%)
Pancreatic carcinoma metastasis (%)	1 (2.9%)

Table 1. Demographic and perioperative characteristics of the included patients. n: number, IQR: interquartile range, BMI: body mass index, MELD-Na score: model for end-stage liver disease, APRI score: AST-to-platelet ratio index, CTP score: Child–Turcotte–Pugh score, ICG-R15: indocyanine green retention rate at 15 min, FLR: future liver remnant, 2D-SWE: two-dimensional shear wave elastography, Metavir score: meta-analysis of histological data in viral hepatitis, HCC hepatocellular carcinoma, IHCC: intrahepatic cholangiocarcinoma.

Total liver filtration (measured by dynamic [^{99m}Tc]Tc-mebrofenin SPECT/CT) was significantly negatively correlated with the MELD-Na score ($\rho = -0.42$, $P = 0.04$) and the ICG-R15 ($\rho = -0.48$, $P = 0.018$). The APRI score was not correlated with the ICG-R15, total liver filtration, or MELD-Na score. CTP was correlated with the MELD-Na score ($\rho = 0.38$, $P = 0.046$) and the ICG-R15 ($\rho = 0.64$, $P = 0.001$) (Fig. 2).

Cases of sufficient FLR when major liver resection was performed as planned

Next, we focused on patients who had a sufficient FLR volume and function to proceed with the planned major liver resection. By evaluating postoperative outcomes in these patients, we aimed to assess the predictive accuracy of our dynamic SPECT/CT measurements for postoperative liver function and complications. This analysis helps in understanding how preoperative FLR assessments can guide surgical decision-making and predict patient outcomes.

In 32/35 patients, the volumetric and/or functional ratio of the FLR was sufficient to perform the planned major liver resection. In 22 patients, the FLR was sufficient according to the first dynamic [^{99m}Tc]Tc-mebrofenin SPECT/CT examination, and in 10 patients, the FLR after parenchymal modulation met the criteria for resection.

Among the 25/32 patients who underwent major liver resection, one patient died intraoperatively due to acute hemodynamic failure. We assessed the postoperative outcomes in the remaining 24 patients. Twelve patients did not develop PHLF, and 8 patients had Grade A PHLF and did not require further intervention. Among those without PHLF, four patients had not received preoperative chemotherapy, eight patients received preoperative chemotherapy, no patients had cirrhosis, and 1 patient experienced postoperative bleeding, which required reoperation. Among the patients with Grade A PHLF, two had cirrhotic livers, and two had previously received chemotherapy.

Four patients developed clinically relevant PHLF according to the ISGLS criteria: two patients with Grade B PHLF and two patients with Grade C PHLF.

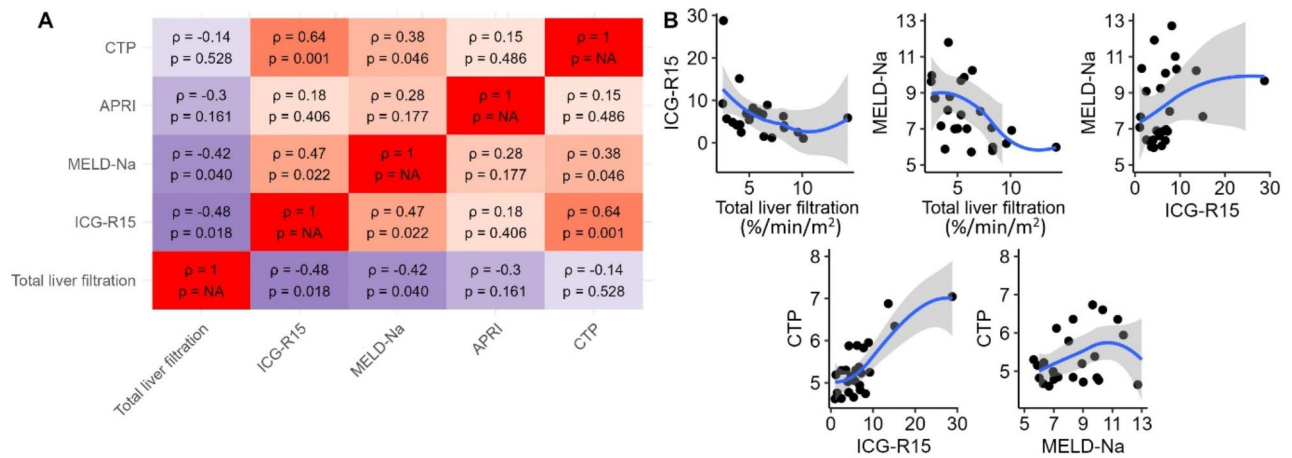


Fig. 2. Correlation matrix for total liver function. **a:** Heatmap showing the Spearman's rank correlation coefficients (ρ) between total liver filtration and preoperative clinical parameters. The color intensity indicates the strength and direction of the correlation. **b:** Scatterplots of the significantly correlated variables with a locally estimated scatterplot smoothing function.

Two patients (2/24) presented with grade B PHLF following right hemihepatectomy. One patient had previously undergone chemotherapy. In these two patients, preoperative parenchymal modulation was not performed because the FLR-V% and FLR-FV% were sufficient.

In another two patients (2/24), Grade C PHLF developed after right trisectionectomy. These two patients experienced the following postoperative complications: segmental hepatic artery occlusion of the remnant liver and heart failure due to postoperative Takotsubo cardiomyopathy. Patient characteristics are shown in Supplementary Table 1.

According to the results of the ROC analysis, FLR filtration was found to be a significant predictor for clinically relevant PHLF (PHLF B + C), with an excellent AUC value (AUC = 0.947, $P = 0.006$). On the basis of the Youden index values, the optimal cut-off value was 2.72%/min/m² (Fig. 3). Some variables showed promising results, such as FLR-FV% (AUC = 0.810) and FLR-V% (AUC = 0.800); however, their efficacy was significant on the basis of the present data set: $p = 0.052$ and 0.063 , respectively. In addition, among the patients who underwent major resection, 21 patients underwent 2D-SWE measurements. FLR stiffness was not a significant predictor of clinically relevant PHLF.

Cases of sufficient FLR when major liver resection was not performed as planned

For 7/32 patients, the preoperative treatment plan was changed despite sufficient FLR-V% and FLR-FV% values. In one patient, intraoperative bisegmentectomy was sufficient according to oncological criteria. Five patients were inoperable due to tumor spread. In one patient, the hemangioma was managed via embolization instead of right hemihepatectomy. Within 90 days, 1/7 patients died because of sepsis, despite the resolution of postoperative biliary leakage. Patient characteristics are shown in Supplementary Table 2.

Patients for whom the planned therapeutic intervention had to be changed due to insufficient FLR

For 3/35 patients, the original surgical plan was changed because the FLR-V% and FLR-FV% values were below the safe limits. However, these patients underwent parenchymal modulation. Thus, two patients were deemed inoperable; one patient underwent segmentectomy combined with thermoablation. The characteristics of the 3 patients are shown in Supplementary Table 3.

The results of the investigation protocol are summarized in Fig. 4.

Effect of parenchymal modulation

Recognizing the importance of parenchymal modulation techniques (such as PVE, PVL, and ALPPS) in increasing FLR, we evaluated their impact on both volumetric and functional liver parameters. By comparing pre- and post-modulation measurements, we aimed to determine the efficacy of these interventions in enhancing liver function as assessed by our dynamic SPECT/CT methodology. This analysis is critical for optimizing preoperative strategies to improve surgical outcomes.

In 13/35 patients without cirrhosis, preoperative parenchymal modulation was performed because of an inadequate FLR after preoperative dynamic [^{99m}Tc]Tc-mebrofenin SPECT/CT. Among these patients, three patients underwent the ALPPS procedure, nine patients underwent portal vein embolization, and one patient underwent portal vein ligation for portal vein occlusion, as it was the chosen parenchymal modulation strategy. Nine of these patients received chemotherapy prior to the parenchymal modulation procedure.

Before parenchymal modulation, the median total liver filtration was 4.99%/min/m² (IQR: 4.37–6.14%/min/m²). After parenchymal modulation, there was a marginal increase of 5.21%/min/m² (IQR: 4.76–6.19%/min/m²).

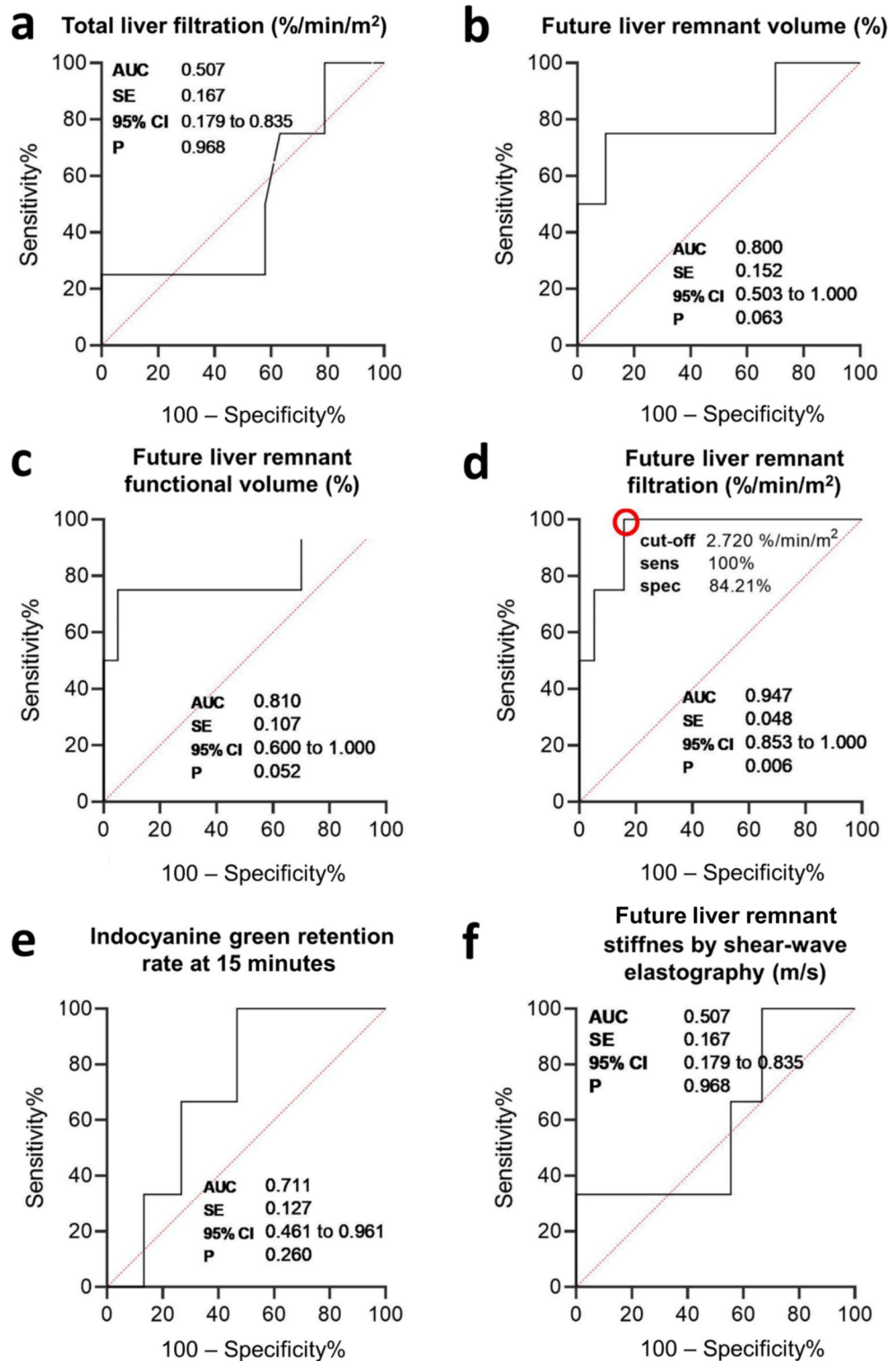


Fig. 3. ROC analyses of liver volumetric and functional parameters to predict clinically relevant PHLF. **a:** Total liver filtration, **b:** FLR volume%, **c:** FLR functional volume%, **d:** FLR filtration, **e:** ICG-R15, **f:** FLR stiffness value. AUC: area under the curve; SE: standard error of the AUC; 95% CI: 95% confidence interval for the AUC; *P*: *P* value; sens: sensitivity; spec: specificity.

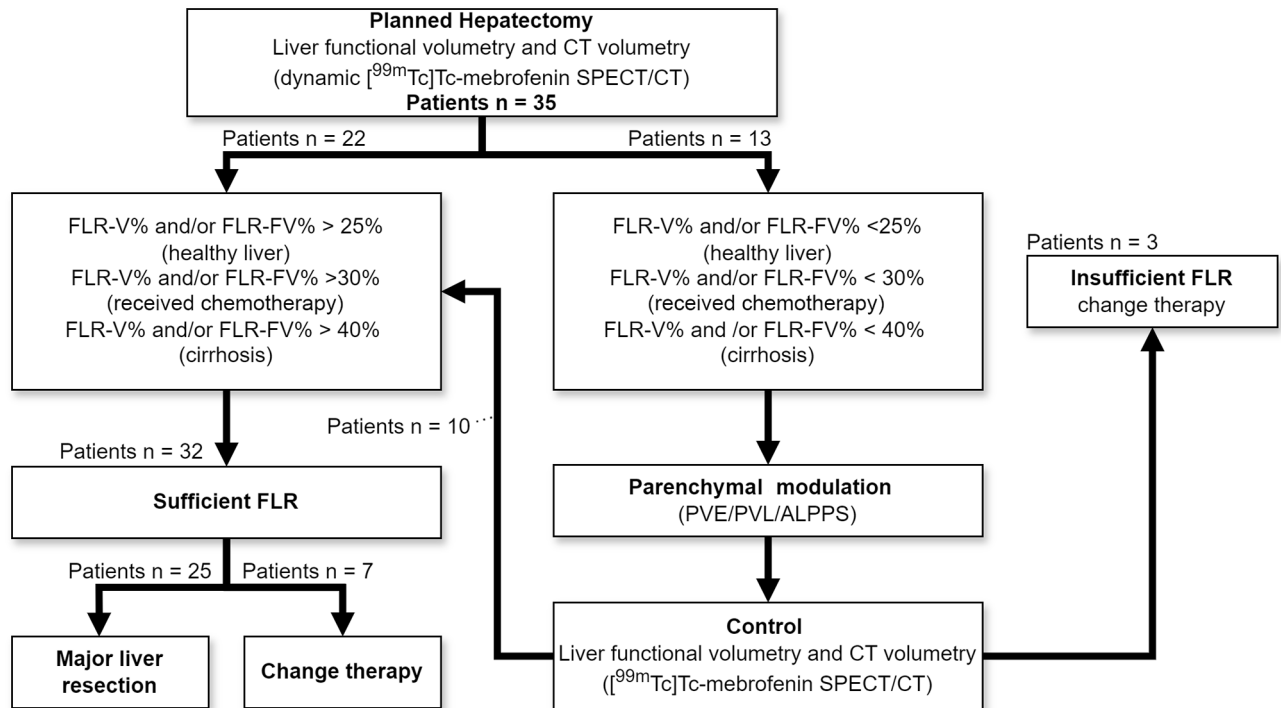


Fig. 4. The results of the investigation protocol. FLR-FV%: future liver remnant functional volume%, FLR-V%: future liver remnant volume%, PVE: portal vein embolization, PVL: portal vein ligation, ALPPS: associating liver partition and portal vein ligation for staged hepatectomy.

in the median filtration. This increase did not appear to be consistent; the IQR regions overlapped significantly, and the difference between the two groups was not significant ($P = 0.88$) (Fig. 5A).

Before modulation, the median FLR-V% was 31.51% (IQR: 24.45–36.60%), whereas after modulation, the median FLR-V% was 46.37% (IQR: 41.01–54.63%). This substantial increase was statistically significant ($P < 0.0001$) (Fig. 5B).

At baseline, the median FLR-FV% was 29.23% (IQR: 21.62–34.23%). Following modulation, a consistent increase to 53.32% (IQR: 46.11–65.25%) was observed. The pronounced increase was statistically significant ($P < 0.0001$) (Fig. 5C).

FLR filtration also increased significantly from a median value of 1.42 (IQR: 0.99–1.77) %/min/m² to 2.79 (IQR: 2.30–3.90) %/min/m² (Fig. 5D).

Finally, after modulation, the median FLR stiffness (measured by ultrasound) increased from 1.37 m/s (IQR: 1.30–1.49 m/s) to 1.47 m/s (IQR: 1.37–1.58 m/s), but the difference was not statistically significant ($P = 0.44$) (Fig. 5E).

In 10/13 patients, the FLR-V% and FLR-FV% increased to a level sufficient to undergo planned hepatectomy, whereas in 3/13 patients, the FLR-V% and FLR-FV% did not increase sufficiently despite parenchymal modulation.

Morbidity and mortality

Twenty-four patients underwent major liver resection, none of whom died within 90 days after surgery. Four patients (4/24 = 17%) had clinically relevant PHLF (Grade B/C), three of whom had not received previous chemotherapy (75%). Patients with Grade C PHLF also experienced postoperative complications.

In general, 35 major morbidities (\geq Clavien–Dindo 3a) occurred in only 5 patients. Two patients developed Grade C PHLF after right trisectionectomy. One patient died intraoperatively, one patient died of sepsis despite resolution of the postoperative biliary leak, and one patient experienced hemorrhaging after right hepatectomy. Two of 35 patients (5.7%) died within 90 days.

Discussion

In our study, functional data were collected during dynamic SPECT acquisition to determine total liver filtration, FLR filtration and FLR functional rates via our new method. Our method makes it possible to detect the distribution of radiopharmaceuticals in 3 dimensions from the beginning of the study. The functional fraction of FLR was determined in the pure parenchymal phase at the same time interval as FLR filtration was calculated. This finding suggests that the functional fraction of FLR determined using this approach may prove to be more accurate than the methodology used in hepatobiliary scintigraphy, which acquires SPECT data later, so intrahepatic and extrahepatic biliary tract activity in the liver should be subtracted¹¹.

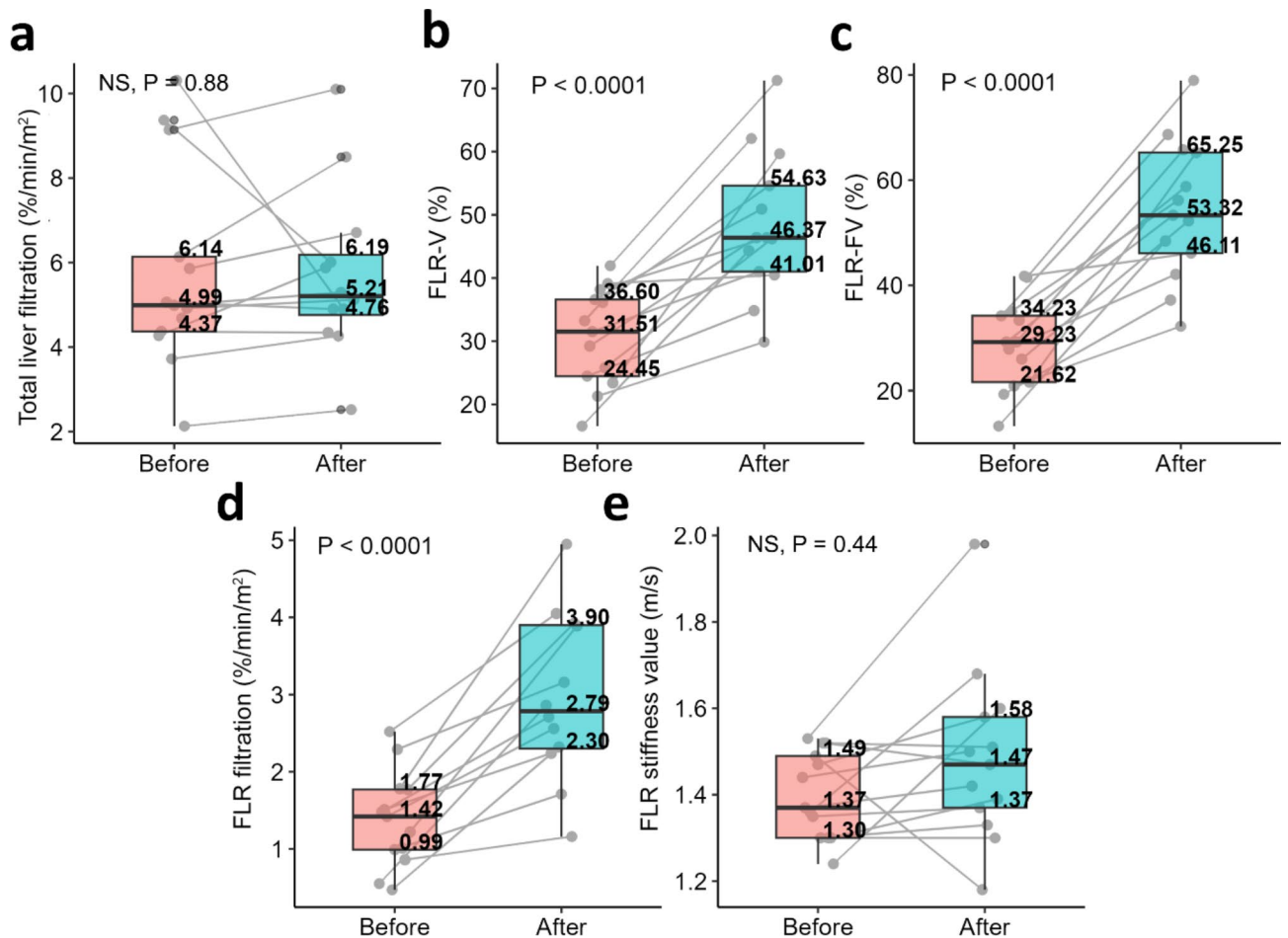


Fig. 5. Effect of parenchymal modulation on various volumetric and functional parameters. In the boxplot, measurement pairs before and after parenchyma modulation are connected by lines. The boxplot is labeled with the median of the measurements and the first and third quartiles. **a:** Total liver filtration, **b:** FLR volume%, **c:** FLR functional volume%, **d:** FLR filtration, **e:** FLR stiffness.

The safe resection limit for the FLR volume fraction depends largely on the presence of any underlying liver disease, so determining total liver function is desirable in preoperative planning. Several liver function tests have been described in the literature. To our knowledge, this was the first study to correlate total liver filtration with several clinical scores and ICG testing. In our study, the Model for End-Stage Liver Disease (MELD)-Na score and the ICG-R15 were significantly negatively to moderately correlated with total liver filtration, as measured by dynamic [^{99m}Tc]Tc-mebrofenin SPECT/CT. The MELD score is based on laboratory parameters (the international normalized ratio (INR), serum creatinine level and serum bilirubin level). The MELD score has been shown to be useful in predicting surgical risk, outcome, and nontransplant surgical mortality²⁴. Dynamic [^{99m}Tc]Tc-mebrofenin SPECT/CT and ICG are dynamic functional methods. ICG is a water-soluble dye that, like mebrofenin, is selectively taken up by liver cells and excreted without metabolism. Several studies have investigated ICG clearance before hepatectomy and revealed that it is a good predictor of global liver function^{25,26}. However, the ICG clearance test measures only total liver function, not segmental function; therefore, no conclusions can be drawn from this measurement about the quality of the FLR, which is a prerequisite for safe major liver resection²⁷. ICG measurement is associated with high drug and equipment costs and is not recommended for patients with thyrotoxicosis²⁸. Mebrofenin is an inexpensive, widely available radiopharmaceutical, but only a few centers use it for preoperative planning before major liver resection¹.

In our study, total liver filtration was not significantly correlated with the Child-Pugh-Turcotte score (CTP). The CTP score was used to identify high-risk patients in our study, who were selected preoperatively according to the inclusion criteria²⁹. The CTP score may remain within normal limits in HCC patients without cirrhosis, despite the presence of significant liver parenchymal disease³⁰. There was no significant correlation between the APRI score and the ICG-R15, total liver filtration, or Meld-Na score in our study. The aspartate aminotransferase-to-platelet ratio index (APRI) score was first described by Wai et al. as a noninvasive marker to assess hepatic fibrosis in patients with chronic hepatitis C virus (HCV) infection. This score is calculated from the AST level and platelet count³¹. The APRI score indicates the probability of fibrosis without measuring the functional capacity of the liver, which can be modeled via dynamic liver function tests.

Preventing mortality from PHLF after major resection is essential. PHLF can have both primary and secondary causes. It is important to preserve adequate functional liver tissue after planned surgery to avoid one of the causes of primary post-hepatectomy liver failure. In this study, resectability was assessed using our algorithm on the basis of the volume and functional fraction of the FLR. In our study, none of the patients who underwent major liver resection died of postoperative liver failure. To our knowledge, this was the first study to use dynamic [^{99m}Tc]Tc-mebrofenin SPECT to determine a functional parameter (FLR filtration) that predicts clinically relevant PHLF (PHLF Grades B + C). The cutoff value for FLR filtration was 2.72%/min/m², which was almost identical to the cutoff value previously established in the literature on hepatobiliary scintigraphy¹¹. Our results are valuable for confirming the findings of previous studies based on hepatobiliary scintigraphy. Patients with Grade A PHLF do not require relevant postoperative clinical care, and they may benefit from the curative effect of resection²¹. Our results revealed that Grade B PHLF patients had lower FLR filtration values than the cut-off value, so parenchymal modulation in these patients could have increased the value of FLR filtration. However, they did not die within 90 days. Both patients with Grade C PHLF underwent parenchymal modulation. In one of the patients with Grade C PHLF, the FLR filtration value was nearly equivalent to the cutoff value (2.69%/min/m²), but segmental hepatic artery occlusion occurred and could therefore be considered multifactorial PHLF. In the other patient with Grade C PHLF, the FLR filtration value was 2.21%/min/m², which was below the cutoff value; furthermore, she developed postoperative Takotsubo cardiomyopathy, so she also had multifactorial causes of liver failure. Patients with Grade C PHLF have postoperative complications, so a secondary cause of PHLF may also be involved³². In our study, the FLR-FV% value was a near-significant marginal value in predicting Grades B and C PHLF, although this value represents a functional fraction. The inclusion of the FLR filtration value in the decision algorithm may allow a more accurate selection of patients who warrant parenchymal modulation. In our study, the ICG-R15 and total liver filtration value did not have significant cutoff values for the prediction of clinically relevant PHLF. This is because it does not include the FLR fraction of the liver in addition to total liver function. There was no significant cut-off value for FLR stiffness measured by two-dimensional ultrasound shear-wave elastography (2D-SWE) for the prediction of clinically relevant PHLF in the present study. Qiu et al. compared the use of 2D-SWE and indocyanine green (ICG) clearance in the preoperative prediction of PHLF in patients undergoing major liver resection in a retrospective study. 2D-SWE could more accurately predict PHLF than the ICG clearance test could³³. Our results showed that since 2D-SWE cannot measure the ratio of the FLR to the total liver, it might be less suitable for predicting clinically relevant PHLF.

In the case of an insufficient FLR functional ratio, it is possible to increase the FLR via parenchymal modulation procedures¹. We investigated the effect of parenchymal modulation preoperatively. In our study, total liver filtration was not significantly different after parenchymal modulation, so global liver function was not reduced by the intervention. The FLR stiffness value was not significantly changed by parenchymal modulation, suggesting the absence of development of a fibrotic process in the FLR. It has previously been shown that 2D-SWE is able to detect fibrosis of the liver parenchyma³⁴. However, the present study revealed that FLR-V%, FLR-FV%, and FLR-filtration were significantly altered, indicating the success of modulation and predicting the ability of the liver to regenerate. Parenchymal modulation procedures resulted in a significant increase in FLR volume and functional fraction. W. de Graaf et al. reported that the functional increase in the FLR may be more pronounced than the volume increase following PVE³⁵. Furthermore, Olthof et al. reported that the ALPPS procedure results in a greater increase in liver volume than in functional growth, with no parallel change in the volume-to-function ratio³⁶. In our study, the volumetric and functional changes also significantly differed. We looked at the effects of three different parenchymal modulation procedures (ALPPS, PVE, and PVL), but we did not examine the volumetric and functional changes according to the different procedures. In ten patients, the increase exceeded the threshold for operability without deterioration in overall liver function, and major liver resection was possible. However, in three patients, parenchymal modulation was unsuccessful: they had insufficient FLR-V% and FLR-FV%, indicating a low regenerative capacity of the liver. For this reason, a change in therapeutic strategy is needed in these patients. Our results suggest that it may be worthwhile to perform functional volumetry prior to parenchymal modulation to gain insight into the dynamic changes that predict the ability to regenerate after surgery.

Limitations of our study include the following: first, the number of patients included in the study was small, and patients with and without liver parenchymal disease were included as well. Second, the shortest possible SPECT acquisition time in our study was 192 s. Using the list mode or values calculated from the shorter SPECT acquisition time, a more accurate fit of the time-activity curve can be obtained, from which even more accurate values can be calculated. Prospective comparative studies with planar hepatobiliary scintigraphy are needed to confirm our results. Further studies are also needed in the future to determine the cutoff for total liver filtration to define normal and impaired liver function. Third, several intraoperative and postoperative factors (hepatic artery thrombosis and Takotsubo syndrome) influence the development of postoperative liver failure, supporting the multifactorial causes of PHLF. Furthermore, only a small proportion of patients were required to undergo future liver remnant modulation.

Conclusion

Total liver filtration, as determined by dynamic [^{99m}Tc]Tc-mebrofenin SPECT/CT, was correlated with global liver function parameters. Determination of future liver remnant filtration by dynamic [^{99m}Tc]Tc-mebrofenin SPECT/CT is the most useful parameter for predicting clinically relevant post-hepatectomy liver failure. This parameter is useful in the selection of liver parenchyma modulation cases. Determining liver fibrosis alone by ultrasound shear-wave elastography does not provide enough information to safely plan major liver resection.

Data availability

All data generated or analyzed during this study are included in this published article and its supplementary information files.

Received: 23 April 2024; Accepted: 26 November 2024

Published online: 05 December 2024

References

- Primavesi, F. et al. E-AHPBA-ESSO-ESSR Innsbruck consensus guidelines for preoperative liver function assessment before hepatectomy. *Br. J. Surg.* **110**, 1331–1347 (2023).
- Kingham, P. T. et al. Hepatic parenchymal preservation surgery: decreasing morbidity and mortality rates in 4,152 resections for malignancy. *J. Am. Coll. Surg.* **220**, 471–479 (2015).
- Morandi, A. et al. Predicting Post-hepatectomy Liver failure in HCC patients: a review of liver function Assessment based on Laboratory tests scores. *Med. (Mex).* **59**, 1099 (2023).
- Ferraioli, G. et al. Liver Ultrasound Elastography: an update to the World Federation for Ultrasound in Medicine and Biology Guidelines and recommendations. *Ultrasound Med. Biol.* **44**, 2419–2440 (2018).
- Guglielmi, A., Ruzzenente, A., Conci, S., Valdegamberi, A. & Iacono, C. How much remnant is enough in liver resection? *Dig. Surg.* **29**, 6–17 (2012).
- Kubota, K. Measurement of liver volume and hepatic functional reserve as a guide to decision-making in resectional surgery for hepatic tumors. *Hepatology* **26**, 1176–1181 (1997).
- Schindl, M. J. The value of residual liver volume as a predictor of hepatic dysfunction and infection after major liver resection. *Gut* **54**, 289–296 (2005).
- Yamanaka, J., Saito, S. & Fujimoto, J. Impact of Preoperative Planning using virtual Segmental Volumetry on Liver Resection for Hepatocellular Carcinoma. *World J. Surg.* **31**, 1251–1257 (2007).
- Okabe, H. et al. Remnant liver volume-based predictors of postoperative liver dysfunction after hepatectomy: analysis of 625 consecutive patients from a single institution. *Int. J. Clin. Oncol.* **19**, 614–621 (2014).
- Makuuchi, M. et al. Surgery for small liver cancers. *Semin Surg. Oncol.* **9**, 298–304 (1993).
- Arntz, P. J. W. et al. Joint EANM/SNMMI/IHPBA procedure guideline for [99mTc]Tc-mebrofenin hepatobiliary scintigraphy SPECT/CT in the quantitative assessment of the future liver remnant function. *HPB* **25**, 1131–1144 (2023).
- Krishnamurthy, G. T. & Turner, F. E. Pharmacokinetics and clinical application of technetium 99m-labeled hepatobiliary agents. *Semin Nucl. Med.* **20**, 130–149 (1990).
- Gullberg, G. T., Reutter, B. W., Sitek, A., Maltz, J. S. & Budinger, T. F. Dynamic single photon emission computed tomography—basic principles and cardiac applications. *Phys. Med. Biol.* **55**, R111–R191 (2010).
- Baumgartner, R. et al. Impact of post-hepatectomy liver failure on morbidity and short- and long-term survival after major hepatectomy. *BJS Open.* **6**, zrac097 (2022).
- Osman, A. M., El Shimy, A. & Abd El Aziz, M. M. 2D shear wave elastography (SWE) performance versus vibration-controlled transient elastography (VCTE/fibroscan) in the assessment of liver stiffness in chronic hepatitis. *Insights Imaging.* ;11(1):38. Published 2020 Mar 10. doi: (2020). <https://doi.org/10.1186/s13244-020-0839-y>
- Bennink, R. J. et al. Preoperative assessment of postoperative remnant liver function using hepatobiliary scintigraphy. *J. Nucl. Med. Off Publ Soc. Nucl. Med.* **45**, 965–971 (2004).
- Rassam, F., Olthof, P. B., Bennink, R. J. & van Gulik T. M. Current modalities for the Assessment of Future Remnant Liver function. *Visc. Med.* **33**, 442–448 (2017).
- Newville, M. et al. Imfit/Imfit-py: 1.2.2. Zenodo (2023). <https://doi.org/10.5281/ZENODO.8145703>
- Ekman, M., Fjälling, M., Friman, S., Carlson, S. & Volkman, R. Liver uptake function measured by IODIDA clearance rate in liver transplant patients and healthy volunteers. *Nucl. Med. Commun.* **17**, 235–242 (1996).
- Mosteller, R. D. Simplified calculation of body-surface area. *N Engl. J. Med.* **317**, 1098 (1987).
- Rahbari, N. N. et al. Posthepatectomy liver failure: a definition and grading by the International Study Group of Liver surgery (ISGLS). *Surgery* **149**, 713–724 (2011).
- Narita, M. et al. What is a safe future liver remnant size in patients undergoing major hepatectomy for colorectal liver metastases and treated by intensive preoperative chemotherapy? *Ann Surg Oncol.* ;19(8):2526–38. doi: (2012). <https://doi.org/10.1245/s10434-012-2274-x>. Epub 2012 Mar 7. PMID: 22395987.
- Clavien, P. A. et al. The Clavien-Dindo classification of Surgical complications: five-year experience. *Ann. Surg.* **250**, 187–196 (2009).
- Northup, P. G., Wanamaker, R. C., Lee, V. D., Adams, R. B. & Berg, C. L. Model for end-stage liver disease (MELD) predicts Nontransplant Surgical mortality in patients with cirrhosis. *Ann. Surg.* **242**, 244–251 (2005).
- Hwang, S. et al. Quantified Risk Assessment for Major Hepatectomy via the Indocyanine Green Clearance Rate and Liver Volumetry Combined with Standard Liver volume. *J. Gastrointest. Surg.* **19**, 1305–1314 (2015).
- Kobayashi, Y., Kiya, Y., Nishioka, Y., Hashimoto, M. & Shindoh, J. Indocyanine green clearance of remnant liver (ICG-Krem) predicts postoperative subclinical hepatic insufficiency after resection of colorectal liver metastasis: theoretical validation for safe expansion of Makuuchi's criteria. *HPB* **22**, 258–264 (2020).
- Dinant, S. et al. Risk Assessment of Posthepatectomy Liver failure using Hepatobiliary Scintigraphy and CT Volumetry. *J. Nucl. Med.* **48**, 685–692 (2007).
- Levesque, E. et al. Current use and perspective of indocyanine green clearance in liver diseases. *Anaesth. Crit. Care Pain Med.* **35**, 49–57 (2016).
- Nonami, T. et al. Blood loss and ICG clearance as best prognostic markers of post-hepatectomy liver failure. *Hepatogastroenterology* **46**, 1669–1672 (1999).
- Johnson, P. J. et al. Assessment of liver function in patients with Hepatocellular Carcinoma: a New evidence-based Approach—the ALBI Grade. *J. Clin. Oncol.* **33**, 550–558 (2015).
- Wai, C. A simple noninvasive index can predict both significant fibrosis and cirrhosis in patients with chronic hepatitis C. *Hepatology* **38**, 518–526 (2003).
- Schreckenbach, T., Liese, J., Bechstein, W. O. & Moench, C. Posthepatectomy Liver failure. *Dig. Surg.* **29**, 79–85 (2012).
- Qiu, T. et al. Comparison between preoperative two-dimensional shear wave elastography and indocyanine green clearance test for prediction of post-hepatectomy liver failure. *Quant. Imaging Med. Surg.* **11**, 1692–1700 (2021).
- Herrmann, E. et al. Assessment of biopsy-proven liver fibrosis by two-dimensional shear wave elastography: an individual patient data-based meta-analysis. *Hepatology* **67**, 260–272 (2018).
- De Graaf, W. et al. Assessment of future remnant liver function using Hepatobiliary Scintigraphy in patients undergoing Major Liver Resection. *J. Gastrointest. Surg.* **14**, 369–378 (2010).
- Olthof, P. B. et al. 99mTc-mebrofenin hepatobiliary scintigraphy predicts liver failure following major liver resection for perihilar cholangiocarcinoma. *HPB* **19**, 850–858 (2017).

Acknowledgements

We thank Anna Mayer and Springer Nature Author Services for linguistic support.

Author contributions

A.B: Data curation, formal analysis, investigation, methodology, visualization, writing and original draft preparation. L.L: Data collection, investigation, review and editing. Sz. U: Data curation, formal analysis, investigation. T.G: collected and reviewed the data. M.B: Data curation, formal analysis, visualization, writing–review and editing. J.H: collected and reviewed the data. Gy. L: review. A.N: Collecting data, review. I.F: Collecting data, review. G.S: Collecting data, review. L.P: methodology, resources, validation, writing – review and editing. Zs. B: Conceptualization, validation, writing–review and editing. All the authors read and approved the final manuscript.

Declarations

Ethics approval and consent to participate

The study was approved by the Local Ethical Committee for Clinical Research at our university (reference no. 123/2022-SZTE RKEB). The study protocol adheres to the ethical guidelines outlined in the 1975 Declaration of Helsinki, as confirmed in prior approval by the institution’s human research committee. Informed consent was obtained from all participating patients.

Competing interests

The authors declare no competing interests.

Additional information

Supplementary Information The online version contains supplementary material available at <https://doi.org/10.1038/s41598-024-81331-z>.

Correspondence and requests for materials should be addressed to A.B.

Reprints and permissions information is available at www.nature.com/reprints.

Publisher’s note Springer Nature remains neutral with regard to jurisdictional claims in published maps and institutional affiliations.

Open Access This article is licensed under a Creative Commons Attribution-NonCommercial-NoDerivatives 4.0 International License, which permits any non-commercial use, sharing, distribution and reproduction in any medium or format, as long as you give appropriate credit to the original author(s) and the source, provide a link to the Creative Commons licence, and indicate if you modified the licensed material. You do not have permission under this licence to share adapted material derived from this article or parts of it. The images or other third party material in this article are included in the article’s Creative Commons licence, unless indicated otherwise in a credit line to the material. If material is not included in the article’s Creative Commons licence and your intended use is not permitted by statutory regulation or exceeds the permitted use, you will need to obtain permission directly from the copyright holder. To view a copy of this licence, visit <http://creativecommons.org/licenses/by-nc-nd/4.0/>.

© The Author(s) 2024